

## Frictional ignition of Ti40 fireproof titanium alloys for aero-engine in oxygen-containing media

Guang-bao MI<sup>1,2</sup>, Xu HUANG<sup>1</sup>, Jing-xia CAO<sup>1</sup>, Chun-xiao CAO<sup>1</sup>, Xiu-song HUANG<sup>2</sup>

1. Aviation Key Laboratory of Science and Technology on Advanced Titanium Alloys,  
Beijing Institute of Aeronautical Materials, Beijing 100095, China;

2. National Center of Novel Materials for International Research, Tsinghua University, Beijing 100084, China

Received 15 August 2012; accepted 29 December 2012

**Abstract:** The effect of friction pressure  $p$  and oxygen concentration  $x_O$  on the fireproof performance of Ti40 titanium alloy was studied by frictional ignition test, the  $p$ – $x_O$  relationship quantitatively describing the fireproof performance of Ti40 was established and the fireproof mechanism of Ti40 was analyzed by SEM, XRD and EDS. The results show that the  $p$ – $x_O$  relationship of Ti40 obeys parabolic rule. The varying range of  $x_O$  is about 25% while  $p$  varies within 0.1–0.25 MPa. When  $x_O$  is  $\geq 70\%$ , Ti40 is ignited immediately at room temperature and develops into continual and steady burning, and the duration of burning is more than 10 s. The fireproof performance of Ti40 is better than TC4 while  $x_O$  of Ti40 is at least 40% higher than TC4. When  $x_O$  is low, the fireproof performance of Ti40 is more sensitive to  $p$ ; when  $x_O$  increases, it is more sensitive to  $x_O$ . The forming of fused oxides of  $V_2O_5$ ,  $TiO_2$  and  $Cr_2O_3$  with strong inner interaction during friction is the basic reason of high fireproof performance of Ti40.

**Key words:** Ti40 fireproof titanium alloys; fireproof performance; fused oxides; fireproof mechanism; titanium fire

### 1 Introduction

High thrust-weight ratio is required for next generation of advanced aero-engine, which contradicts the increasing tendency of titanium fire of titanium components in the compressor. New titanium alloys with high temperature resistance and fire resistance are urgently needed [1]. As new high temperature titanium alloys, fireproof titanium alloys with excellent fire resistance are becoming a promising and critical material for advanced aero-engine. Alloy C (Ti–V–Cr type) and BTT-1, 3 (Ti–Cu–Al type) fireproof titanium alloys were developed by America and Russia, respectively [2,3]. Based on Alloy C, Ti40 (Ti–25V–15Cr–0.2Si) and BuRTi (Ti–25V–15Cr–2Al–0.2C) were developed by China and England, respectively [4–6].

The boundary between ignition and no ignition of Alloy C under different conditions of gas flow pressure and temperature was determined by  $CO_2$  laser ignition apparatus by America and the ignition temperature of Alloy C was found 500 °C higher than that of TC4 under

345 kPa gas flow pressure, which provided a powerful basis for the use of Alloy C in the fourth-generation fighter engine F119. This alloy, with a highest working temperature of 540 °C, was used for castings and blades in the compressor and exhaust nozzle, etc [7,8]. The fireproof performance of titanium alloys such as BTT-1 and BTT-3 was also studied by frictional ignition apparatus by Russia, concluding that the ignition temperature followed the relation BTT-3>BTT-1>BT15>BT23>BT25 and the ignition temperature of BTT-1 was 650 °C. These results provided the basis for trial runs of BTT-1 in an engine. This alloy, with highest working temperature of 450 °C, was used for castings and blades in the compressor [9]. From the later period of “the 8th-Five Year Plan”, China also explored the fireproof titanium alloys. Direct current simulation burn (DCSB) method was applied to studying the burning rate of Ti40 by Northwest Institute for Nonferrous Metal Research, concluding that the burning rate of Ti40 was lower than that of TC4, which promoted the application of Ti40 [10]. However, comparing to foreign researches, the basic experimental and theoretical studies on

fireproof titanium are not adequate, such as fireproof mechanism and the boundary between ignition and no ignition. The shortage of studies results in uncertainty of fireproof level of titanium alloys used in the aero-engine and restricts the material selection of fireproof titanium alloys for engine designers.

Titanium fire in the aero-engine is a typical accident due to forced ignition. The high-energy friction or load impact between the blade and casting leads to ignition. If titanium alloys are ignited, the components in the compressor burn continually only for 4–20 s under the gas flow with high temperature and pressure. The burning time is too short to take extinguishing measures. Thus, to prevent titanium fire effectively, the fireproof performance of Ti40 was evaluated by frictional ignition test and was compared to the ordinary titanium alloys in this study, providing key performance parameters and technical reference for the application of fireproof titanium alloys in the advanced aero-engine.

## 2 Experimental

The Ti40 alloy was fabricated by consumable vacuum arc melting, sheathed extrusion, forging and rolling. The TC4 for comparison was taken from a die forging part. The fireproof performance was evaluated by frictional ignition test, whose schematic diagram is shown in Fig. 1 [11]. The test samples consisted of a wedge-shaped sample A with thickness of 2–3 mm and a strip sample B. The sample A was mounted to a rotating shaft which was connected to a drive motor and the sample B was mounted by a fixture. After the electrical system and gas supply system started, under certain combination of friction pressure and pre-set oxygen/air mixture flow, the high-speed rotating sample A and the fixed sample B formed a friction pair and the samples were ignited due to violent friction. Whether ignition happens or not can be judged by the recording of the process and the morphology of the sample after the test. The rotating speed of sample A was 5000 r/min and the

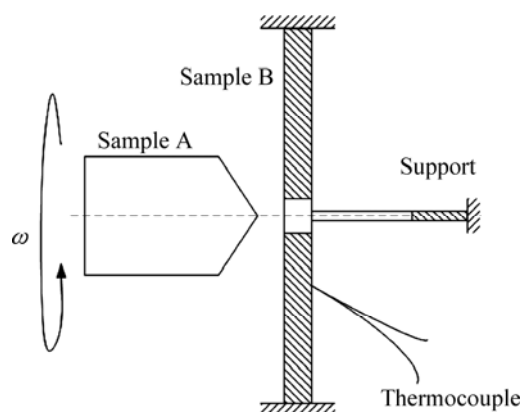


Fig. 1 Schematic diagram of frictional ignition apparatus

pressure of gas flow was 0.1 MPa. The initial temperature of samples was constant. The friction pressure  $p$  and the oxygen concentration  $x_O$  of the pre-mixed gas were adjustable parameters. The samples of ignition and no ignition after tests were analyzed by XRD, SEM and EDS, etc.

## 3 Results and discussion

The test results of frictional ignition of Ti40 are shown in Fig. 2. The red solid circular point indicates that ignition happens under the condition of  $(p, x_O)$ , while the black hollow circular point refers to no ignition. By data processing, difference iteration and nonlinear fitting, the  $p$ – $x_O$  relationship of Ti40 is given, which obeys parabolic rule:

$$p = -0.91 + 0.03x_O - 2.36 \times 10^{-4} x_O^2 \quad (1)$$

where  $p$  is the friction pressure, MPa;  $x_O$  is the oxygen concentration, %.

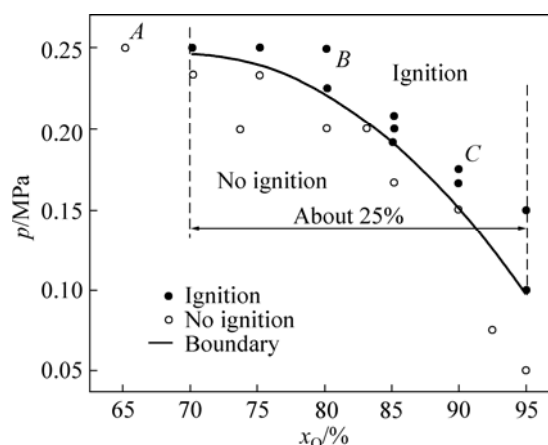


Fig. 2 Test results of frictional ignition of Ti40 and relationship of  $p$ – $x_O$

Equation (1) describes the boundary between ignition and no ignition (see the curve  $p$ – $x_O$  in Fig. 2), showing that  $p$  decreases with  $x_O$  by parabolic law. Thus, the relationship  $p$ – $x_O$  directly reflects the resistance of Ti40 to frictional ignition under the conditions in this experiment. That is,  $p$ – $x_O$  characterizes the frictional fireproof performance of Ti40 (hereinafter, fireproof performance).

From Fig. 2, the varying range of  $x_O$  is about 25% while  $p$  varies within 0.1–0.25 MPa, showing that the fireproof performance has different sensitivity with  $x_O$  and  $p$ . When  $x_O$  is low, the fireproof performance of Ti40 is more sensitive to  $p$ ; when  $x_O$  increases, the fireproof performance is more sensitive to  $x_O$ . It can be deduced that under air condition containing low oxygen, the fireproof performance of Ti40 is mainly controlled by friction pressure.

By observing the frictional ignition process and the morphology of sample B after the test, the fireproof performance of Ti40 is further discussed. The recordings of the processes corresponding to the points A, B and C (Fig. 2) are shown in Figs. 3, 4 and 5, respectively. In terms of point A, when the high-speed rotating sample A contacts with the hole of sample B, the violent friction sparks appear (Fig. 3(a)). As the rubbing continues, the sample temperature increases sharply, appearing red-hot state (Fig. 3(b)). After rubbing for 5 s, the sample A separates from the sample B. The red-hot state of sample B disappears rapidly 3–4 s after the friction ends (Fig. 3(c)). The early rubbing processes corresponding to points B and C are similar to those of point A, except that the sample B is ignited after rubbing for 4–5 s (Figs. 4(a), 5(a)). After separation between samples A and B, the sample B burns continually, which is more violent for point C (Figs. 4(b) and 5(b)). The duration of burning for point C is about twice as long as that for point B

(Figs. 4(c) and 5(c)). It can be found that under the conditions in this experiment, when  $x_0$  is smaller than the critical value, even if  $p$  reaches the maximum, the sample B can not be ignited. When  $x_0$  exceeds the critical value, the sample B is ignited and keeps burning for tens of seconds. This also indicates that Ti40 would soon develop into continual and steady burning after ignition.

The morphologies of Ti40 sample B after the test under abovementioned three conditions are shown in Fig. 6. From Fig. 6, due to the heat generated by friction between the samples A and B, a heat-affected zone I appears near the hole of sample B. The area of heat-affected zone increases from point A to point C, the same as the changing rule of duration of burning. Under condition (a), no evidence shows that the sample B is ignited. Due to the formation of liquid metal during friction, the pre-machined hole in sample B is filled with the metal, as zone II shown in Fig. 6(a). Under conditions (b) and (c), a big irregular hole forms at the

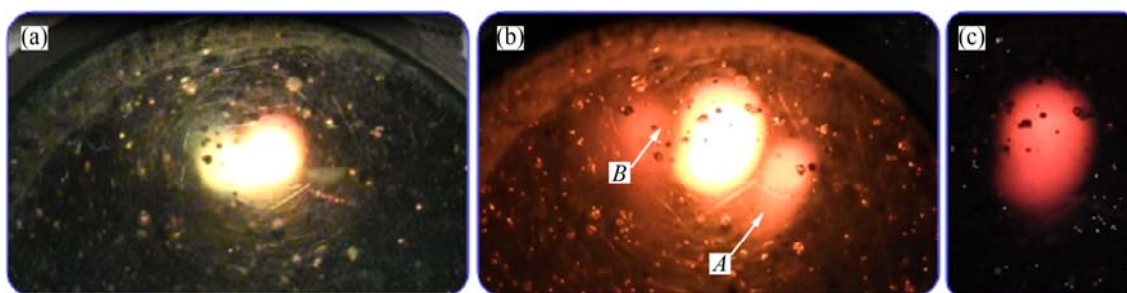


**Fig. 3** Recordings of frictional ignition process of Ti40 under condition of  $p=0.25$  MPa and  $x=65\%$  at point A in Fig. 2: (a) After rubbing for 1 s; (b) After separation between samples A and B; (c)  $x=3-4$  s after rubbing ended

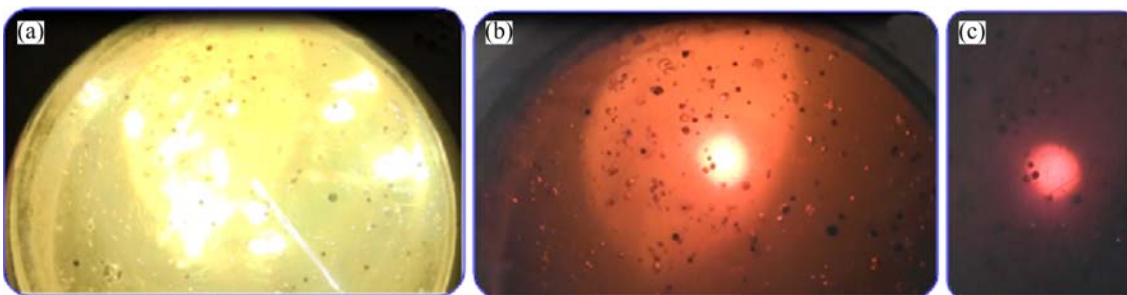


**Fig. 4** Recordings of frictional ignition process of Ti40 under condition of  $p=0.25$  MPa and  $x=80\%$  at point B in Fig. 2: (a) After rubbing for 4–5 s, sample B was ignited; (b) Sample B burning for 7–8 s; (c) After burning for 11 s, sample B extinguished

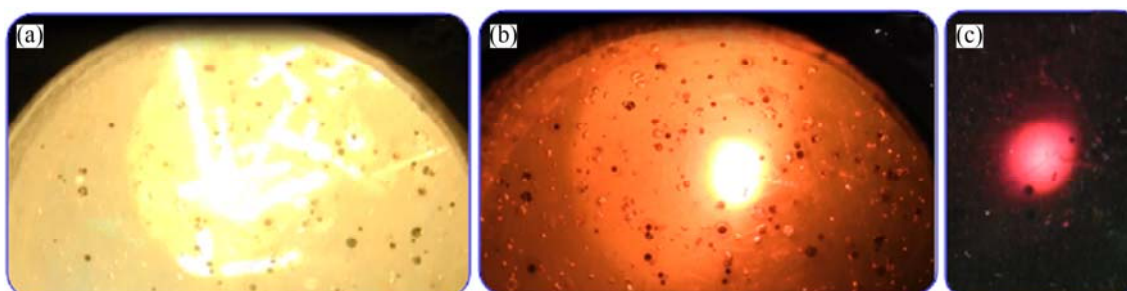


**Fig. 5** Recordings of frictional ignition process of Ti40 under condition of  $p=0.175$  MPa and  $x=90\%$  at point C in Fig. 2: (a) After rubbing for 4–5 s, sample B was ignited; (b) Sample B burns for 11–12 s; (c) After burning for 22–23 s, sample B extinguished

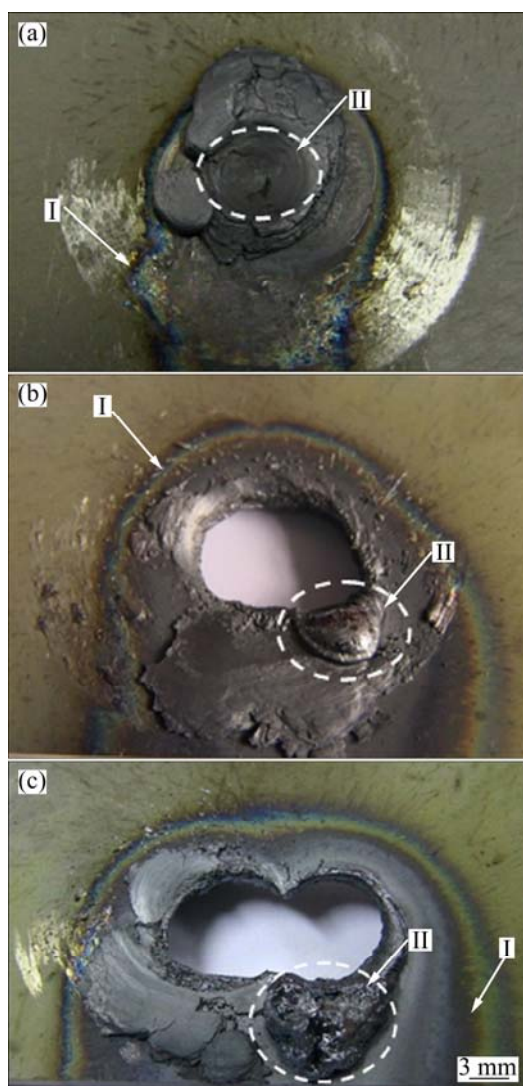


**Fig. 6** Morphologies of Ti40 sample B after test under three conditions: (a)  $p=0.25$  MPa,  $x=65\%$ ; (b)  $p=0.25$  MPa,  $x=80\%$ ; (c)  $p=0.175$  MPa,  $x=90\%$

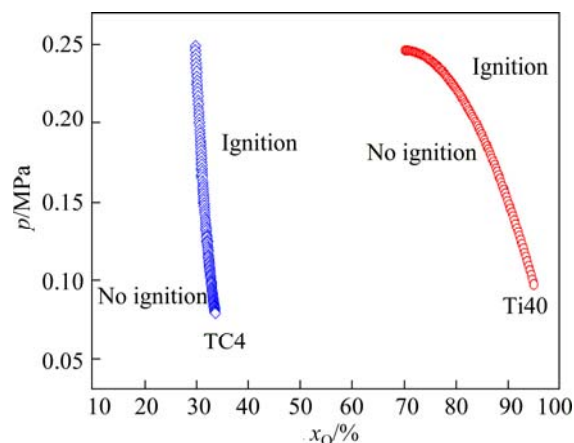
position of initial hole, as a result of continually burning of sample B after igniting by friction. Along with the gas flow direction, a raised zone II forms due to the flow of liquid metal driven by gas flow during burning, as shown in Figs. 6(b) and (c).

Similarly, based on the test points of ignition and no ignition of TC4 under different conditions of ( $p$ ,  $x_O$ ), the relationship  $p-x_O$  describing the fireproof performance of TC4 is obtained, as shown in Fig. 7. The curve obeys parabolic rule as

$$p=8.31-0.47x_O+6.74\times 10^{-3}x_O^2 \quad (2)$$

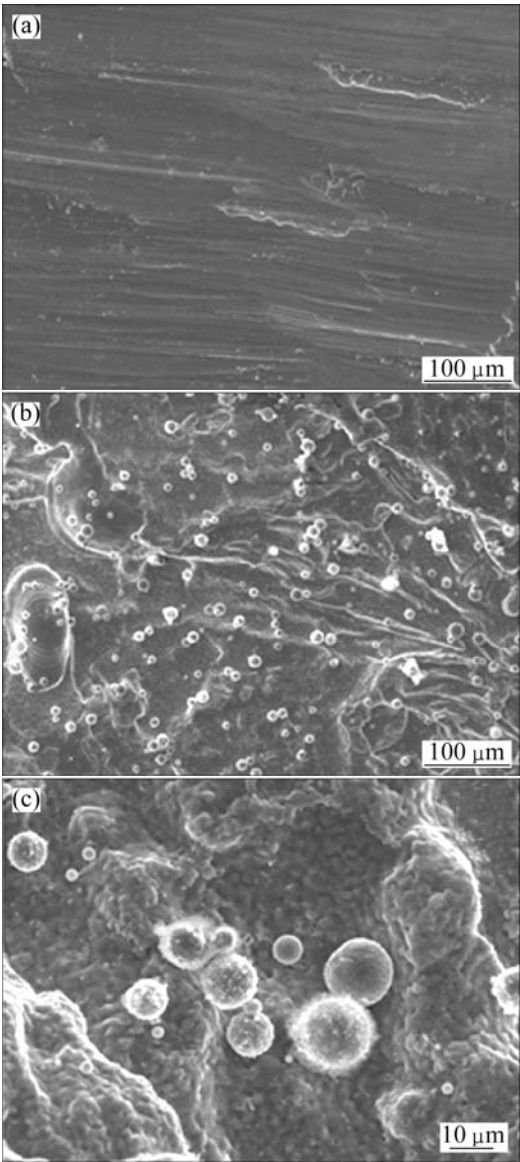
From Fig. 7 and Eq. (2), the varying range of  $x_O$  is about 4% while  $p$  varies within 0.075–0.25 MPa. It indicates that the fireproof performance of TC4 is sensitive to oxygen concentration, but not friction

pressure. The oxygen concentration  $x_O$  is the main factor influencing fireproof performance of TC4. The relationship  $p-x_O$  is also shown in Fig. 7. By comparison, the fireproof performance of Ti40 is much better than TC4. In this test, the oxygen concentration required for ignition of Ti40 is at least 40% higher than TC4.



**Fig. 7** Fireproof performances of Ti40 and TC4

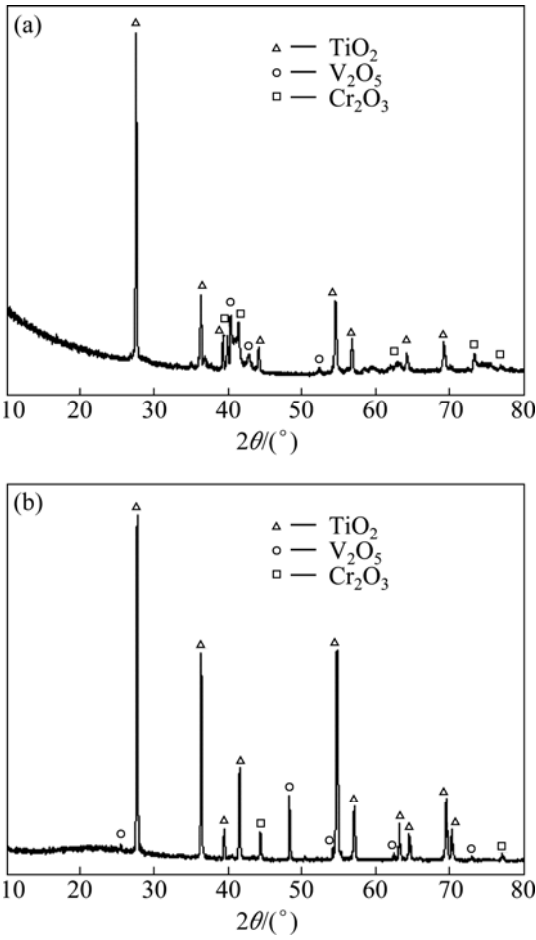
By analyzing the products of the samples of ignition and no ignition, the fireproof mechanism of Ti40 is discussed. The SEM results of Ti40 products after frictional ignition test are shown in Fig. 8. The product surface of no ignition appears smooth and black with obvious friction marks (Fig. 8(a)). The product surface of ignition is rough with dispersed spherical particles (Fig. 8(b)). These particles attach to the product surface and are not generated from the liquid metal directly (Fig. 8(c)). By XRD analysis, it is found that the product surface of no ignition consists of three phases  $V_2O_5$ ,  $TiO_2$  and  $Cr_2O_3$  (Fig. 9(a)), the same as phases of the particles on the surface of the product of ignition (Fig. 9(b)). The contents of Ti, V, Cr and O in particles were analyzed by EDS, as listed in Table 1. The content of  $Cr_2O_3$  is lower than that of  $V_2O_5$  and  $TiO_2$ , and the content of O element is high. Based on molecular cluster physical model of vapor condensation [12], these particles are believed to form due to the rapid condensation of vapour during friction. Because the particles do not only consist of  $V_2O_5$  condensed from vapour, but also fused oxides. It can be judged that the three oxides have strong interaction even for the clusters in the oxide vapour, showing the complementarity and compatibility between the “softening phase” and “hard phase” of the three oxides. This binding force among the oxides originates from the strong interaction among the electrons in conduction band in 3d orbitals of Ti, V and Cr, and also between the electrons in valence band in 2p orbital of O and the electrons in conduction band in 3d orbitals of V



**Fig. 8** SEM images of surface of Ti40 products: (a) No ignition; (b) Ignition; (c) Spherical particles

and Cr [13–15]. Based on the discussion above, the fireproof mechanism of Ti40 can be concluded. During high-speed friction, a layer of fused oxides of  $V_2O_5$ ,  $TiO_2$  and  $Cr_2O_3$  on the sample surface forms quickly (layer thickness of 2–5  $\mu m$  and densely binding between layer

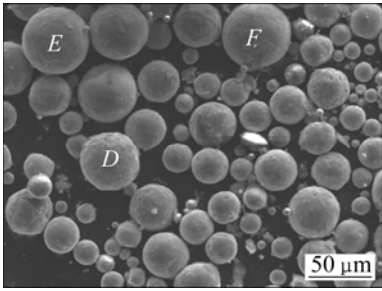
and substrate, as shown in Fig. 10). On one hand, the first-formed “softening phases” liquid  $V_2O_5$  bridges the defects in the “hard phases”  $TiO_2$  and  $Cr_2O_3$ , which releases the stress in the oxides, leading to improvement of the compactness of the oxides and binding force to the alloy substrate; meanwhile, the oxygen diffusion rate slows down. On the other hand, the formation of fused oxides improves the lubricating condition by translating dry friction into wet friction, leading to frictional coefficient, frictional force and frictional heat decreasing, which is similar to that matches cannot be ignited under wet condition.



**Fig. 9** XRD patterns of burning products of Ti40: (a) No ignition; (b) After ignition

**Table 1** EDS results of burning products of Ti40

Element	Point <i>D</i>		Point <i>E</i>		Point <i>F</i>		Average value	
	w/%	x/%	w/%	x/%	w/%	x/%	w/%	x/%
Ti	46.31	25.96	49.67	28.56	42.61	22.77	46.20	25.76
O	36.42	61.13	34.62	59.60	41.05	65.68	37.36	62.14
V	11.89	6.27	11.36	6.14	12.36	6.21	11.87	6.21
Cr	2.82	1.46	2.29	1.21	1.92	0.95	2.34	1.21



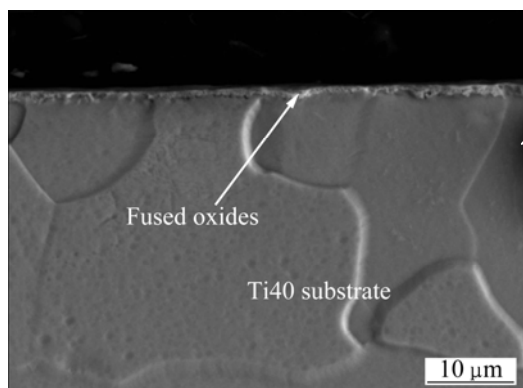


Fig. 10 SEM image showing layer of fused oxides of  $V_2O_5$ ,  $TiO_2$  and  $Cr_2O_3$  on surface of Ti40

#### 4 Conclusions

1) The relationship  $p-x_0$  quantitatively describing the fireproof performance is established, showing that  $p$  decreases with  $x_0$  by parabolic law. The varying range of  $x_0$  is about 25% while  $p$  varies within 0.1–0.25 MPa. When  $x_0$  is  $\geq 70\%$ , Ti40 is ignited immediately and burns continually and stably, and the duration of burning is more than 10 s.

2) The fireproof performance of Ti40 is better than TC4, while the  $x_0$  of Ti40 is at least 40% higher than TC4. When  $x_0$  is low, the fireproof performance of Ti40 is mainly controlled by  $p$ ; when  $x_0$  increases, it is more sensitive to  $x_0$ , the fireproof performance of TC4 is mainly controlled by  $x_0$ .

3) During high-speed friction, a layer of fused oxides of  $V_2O_5$ ,  $TiO_2$  and  $Cr_2O_3$  on the sample surface forms quickly (layer thickness of 2–5  $\mu m$ ). The three oxides bind firmly, showing the complementarity between the “softening phase” and “hard phase”, which is the basic reason of high fireproof performance of Ti40.

#### References

- [1] MI Guang-bao, HUANG Xiu-song, LI Pei-jie, CAO Jing-xia, HUANG Xu, CAO Chun-xiao. Non-isothermal oxidation and ignition prediction of titanium-chromium alloys [J]. Transactions of Nonferrous Metals Society of China, 2012, 22(10): 2409–2415.
- [2] BERCZIK D M. Age hardenable beta titanium alloy [P]. United States Patent, No. 5176762, 1993.
- [3] BORISOVA YE A, SKLYAROV N M. Fireproof titanium alloys [J]. Physical Metallurgy: New Alloys, 1993 (6): 21–24. (in Russian)
- [4] ZHAO Y Q, ZHU K Y, QU H L, WU H. Microstructures of a burn resistant highly stabilized titanium alloy [J]. Materials Science and Engineering A, 2000, 282: 153–157.
- [5] VOICE W. Use of burn resistant titanium alloy (BurTi) [C]//Xi'an International Titanium Conference. Xi'an, 2005: 39–42.
- [6] LÜTJERING G, WILLIAMS J C. Titanium [M]. 2nd ed. New York: Springer Berlin Heidelberg, 2007: 181–203.
- [7] ANDERSON V, MANTY B. Titanium alloy ignition and combustion [R]. Warminster, PA: Naval Air Development Center Report No. NADC 76083-30, 1978.
- [8] HUANG Xu, CAO Chun-xiao, MA Ji-min, WANG Bao, GAO Yang. Titanium combustion in aeroengines and fire-resistant titanium alloys [J]. Journal of Materials Engineering, 1997(8): 11–15. (in Chinese)
- [9] БОРИСОВА Е А, СКЛЯРОВ Н М. Авиационные материалы и технологии: Горение и пожаробезопасность титановых сплавов [M]. Москва: ВИАМ, 2002: 1–87. (in Russian)
- [10] ZHAO Yong-qing, ZHOU Lian, WANG Xiao, DENG Ju, ZHU Kang-ying, ZHAO Xiang-miao. A method for testing burning velocity of titanium alloy: Chinese Patent, No.9810128.7 [P]. 1998.
- [11] MI Guang-bao, HUANG Xu, CAO Jing-xia, WANG Bao, CAO Chun-xiao. A test method characterizing the fireproof performance of titanium alloys for aero-engine: Chinese Patent, No.201218003649.0 [P]. 2012.
- [12] SONG T Y, LAN Z, MA X H, BAI T. Molecular clustering physical model of steam condensation and the experimental study on the initial droplet size distribution [J]. International Journal of Thermal Sciences, 2009, 48: 2228–2236.
- [13] CHEN Jun, YAN Fei-nan, LIANG Li-ping, LIU Ting-yu, GENG Tao. First-principles study on the optical properties of Cr-doped anatase  $TiO_2$  [J]. Journal of Synthetic Crystals, 2011, 40(3): 758–762. (in Chinese)
- [14] PENG Li-ping, XIA Zheng-cai, YIN Jian-wu. First-principles calculation of rutile and anatase  $TiO_2$  intrinsic defect [J]. Acta Physica Sinica, 2012, 61(3): 037103. (in Chinese)
- [15] HURLEN T. On the defect structure of rutile [J]. Acta Chemica Scandinavica, 1959, 13(2): 365–376.

## 含氧环境中航空发动机用 Ti40 阻燃钛合金的摩擦点燃

弭光宝<sup>1,2</sup>, 黄旭<sup>1</sup>, 曹京霞<sup>1</sup>, 曹春晓<sup>1</sup>, 黄秀松<sup>2</sup>

1. 北京航空材料研究院 先进钛合金航空科技重点实验室, 北京 100095;

2. 清华大学 新材料国际研发中心, 北京 100084

**摘要:** 采用摩擦点燃的方法, 研究摩擦压力  $p$  和氧浓度  $x_0$  对 Ti40 阻燃钛合金的抗点燃性能的影响, 建立了定量描述 Ti40 钛合金抗点燃性能的  $p-x_0$  关系曲线, 并结合 SEM、XRD 和 EDS 等测试手段分析 Ti40 钛合金的抗点燃机理。结果表明: Ti40 钛合金的  $p-x_0$  关系曲线符合抛物线规律,  $p$  在 0.1–0.25 MPa 变化时,  $x_0$  的变化范围约为 25%。当  $x_0 \geq 70\%$  时, Ti40 钛合金在室温条件下即会被点燃, 并迅速发展为持续的稳定燃烧, 且时间长于 10 s。Ti40 钛合金的抗点燃性能优于 TC4 钛合金的, Ti40 合金被点燃时所对应的  $x_0$  至少比 TC4 高 40%。当  $x_0$  较低时, Ti40 钛合金的抗点燃性能对  $p$  较为敏感, 而随着  $x_0$  的增大, 抗点燃性能对  $x_0$  更加敏感。摩擦表面形成的具有强相互作用的  $V_2O_5$ 、 $TiO_2$  和  $Cr_2O_3$  氧化物融合物是 Ti40 钛合金的抗点燃性能提高的根本原因。

**关键词:** Ti40 阻燃钛合金; 抗点燃性能; 氧化物融合物; 抗点燃机理; 钛火

(Edited by Jing-hua FANG)